



THEORETICAL IMPROVEMENT OF THE PLANETARY GEAR DYNAMIC MODEL

Tale Geramitcioski and Ljupco Trajceovski

Keywords: Planetary gear, vibration, dynamic model, mesh stiffness

1. Introduction

Planetary gear and vibration are primary concerns in their applications in helicopters, automobiles, aircraft engines, heavy machinery and marine vehicles. Dynamic analysis's essential to the noise and vibration reduction. This work investigates some critical issues and advances the understanding of planetary gear dynamics.

A lumped-parameter model is built for the dynamic analyses of general planetary gear. The unique properties of natural frequency spectra and vibration modes are rigorously characterized. These special structures apply for general planetary gears with cyclic symmetry and, in practically important case, systems with diametrically opposed planets.

For different analyses purposes, there are several modelling choices such as a simple dynamic factor model, compliance tooth model, torsion model, and geared rotor dynamic model. According to the source-path-receiver relationship between the planetary gear, bearing/mounting, and the cabin different boundaries can be selected for building model. This study focuses on the understanding of planetary gear dynamic behaviour, so a single stage gearset with discrete elements is the basic model for investigation. In previous lumped-parameter models (Cunliffe et al., (1974); Botman (1976); Kahraman, (1994)) the gyroscopic effects caused by carrier rotation have not been considered. Because planetary gears have planets mounted on the rotating carrier, the Coriolis and centripetal accelerations caused by the carrier rotation introduce gyroscopic terms into the system model. For high-speed applications such as aircraft engines (30000 rpm), gyroscopic effects may heavily impact the system stability and behavior. In this study is developed a planetary gear model including the gyroscopic effects, contact loss nonlinearly, mesh stiffness variation and static transmission error excitation. Despite the use of the term planetary gear, this model is applicable for epicyclical gears with any configuration (fixed/floating sun, ring, and carrier, and non-equally spaced planets.).

2. Planetary gear modelling

Lumped-parameter modelling is used in this paper for dynamic analyses. All gears are considered as rigid bodies and component supports are modelled by springs. Linear models with constant stiffness were used by Cunliffe(1974) and Botman (1976). Kahraman derived a more general model with non-linear, time-varying stiffness (1994) for planetary gears with any number and position of planets. He subsequently extended it to three-dimensions for helical gear, and reduced it to a purely torsional one. The planetary gear model used in our analyses is shown in Figure 1. Each component has three degrees of freedom: two translations and one rotation. Kahraman (1994) similarly to that uses the model with two distinctions: (1) the planet deflections are described by radial and tangential coordinates and (2) gyroscopic effects induced by carrier rotation are modelled. The radial and tangential coordinates more naturally describe the vibration modes. Gyroscopic effects in high-speed applications such as aircraft engines may dramatically alter the dynamic behaviour from that at lower

speeds. The coordinates illustrated in Figure 1 are used. The carrier, ring and sun translations $x_h, y_h, h=c,r,s$ and planet translations $z_n, h_n, n=1, \dots, N$ are measured with respect to a rotating frame of \mathbf{r} reference $\mathbf{i}, \mathbf{j}, \mathbf{k}$ fixed to the carrier with origin \mathbf{o} . The $x_h, y_h, h=c,r,s$ are directed towards the equilibrium position of planet 1, and z_n, h_n are the radial and tangential deflections of the n -th planet. The basis $\mathbf{i}, \mathbf{j}, \mathbf{k}$ rotates with the constant carrier angular speed \mathbf{W}_c . The rotational coordinates are $u_h = r_h \mathbf{q}_h, h=c,r,s, 1, \dots, N$, where \mathbf{q}_h is the component rotation; r_h is the base circle radius for sun, ring and planet, and the radius of circle passing through the planet centers for the carrier. Circumferential planet locations are specified by the fixed angles \mathbf{y}_n , where \mathbf{y}_n is measured relative to the rotating basis vector \mathbf{i} so that $\mathbf{y}_n = 0$.

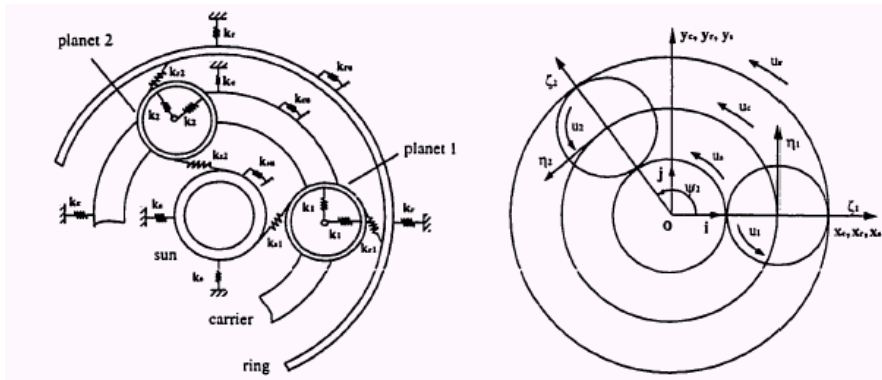


Figure 1. Planetary gear model

As an example, derivation of the sun equations of motion is presented. Figure 2 shows a sun-planet mesh with masses m_s, m_p and moments of inertia I_s, I_p . α_s is the pressure angle of the sun planet mesh. Static transmission error of the n -th sun-planet mesh $e_{sn}(t)$ is included as dynamic excitation at the mesh spring.

$$\ddot{\mathbf{r}}_s = \left(\ddot{x}_s - 2\Omega_c \dot{y}_s - \Omega_c^2 x_s \right) \mathbf{i} + \left(\ddot{y}_s + 2\Omega_c \dot{x}_s - \Omega_c^2 y_s \right) \mathbf{j} \quad (1)$$

The sun position and acceleration are $\mathbf{r}_s = x_s \mathbf{i} + y_s \mathbf{j}$ and

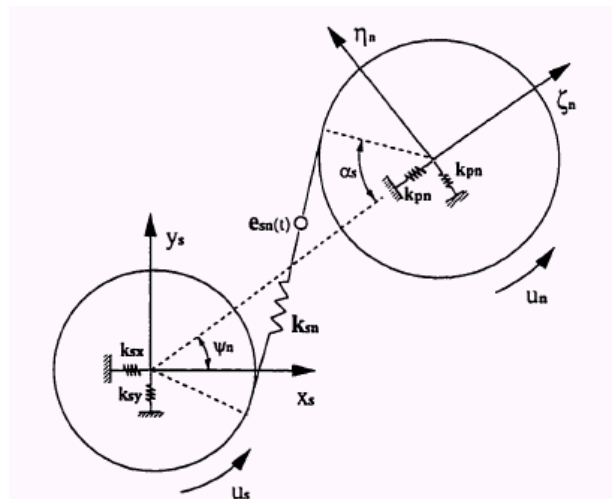


Figure 2. A sun-planet mesh

The equations of motion for the sun are

$$\begin{aligned}
& m_s (\ddot{x}_s - 2\Omega_c \dot{y}_s - \Omega_c^2 x_s) - \sum k_{sn} \mathbf{d}_{sn} \sin \mathbf{y}_{sn} + k_s x_s = 0 \\
\text{Sun :} \quad & m_s (\ddot{y}_s - 2\Omega_c \dot{x}_s - \Omega_c^2 y_s) - \sum k_{sn} \mathbf{d}_{sn} \cos \mathbf{y}_{sn} + k_s y_s = 0 \\
& (I_s / r_s^2) \ddot{u}_s + \sum k_{sn} \mathbf{d}_{sn} + k_{su} u_s = T_s / r_s
\end{aligned} \tag{2}$$

Where the summation index n ranges from 1 to N throughout this study unless otherwise indicated. \mathbf{d}_{sn} defined in (6), denotes the compression of the n -th sun-planet mesh spring. $\mathbf{y}_{sn} = \mathbf{y}_n - \mathbf{a}_s \mathcal{T}_s$ is the torque applied to sun.

The equations of motion for the ring, carrier and n -th planets are obtained similiary.

$$\begin{aligned}
& m_r (\ddot{x}_r - 2\Omega_c \dot{y}_r - \Omega_c^2 x_r) - \sum k_{rn} \mathbf{d}_{rn} \sin \mathbf{y}_{rn} + k_r x_r = 0 \\
\text{Ring} \quad & m_r (\ddot{y}_r - 2\Omega_c \dot{x}_r - \Omega_c^2 y_r) - \sum k_{rn} \mathbf{d}_{rn} \cos \mathbf{y}_{rn} + k_r y_r = 0 \\
& (I_r / r_r^2) \ddot{u}_r + \sum k_{rn} \mathbf{d}_{rn} + k_{ru} u_r = T_r / r_r
\end{aligned} \tag{3}$$

$$\begin{aligned}
& m_c (\ddot{x}_c - 2\Omega_c \dot{y}_c - \Omega_c^2 x_c) - \sum k_p (\mathbf{d}_{nr} \cos \mathbf{y}_n - \mathbf{d}_{nt} \sin \mathbf{y}_n) + k_c x_c = 0 \\
\text{Carrier :} \quad & m_c (\ddot{y}_c - 2\Omega_c \dot{x}_c - \Omega_c^2 y_c) - \sum k_p (\mathbf{d}_{nr} \sin \mathbf{y}_n + \mathbf{d}_{nt} \cos \mathbf{y}_n) + k_c y_c = 0 \\
& (I_c / r_c^2) \ddot{u}_c + \sum k_p \mathbf{d}_{nt} + k_{cu} u_c = T_c / r_c
\end{aligned} \tag{4}$$

$$\begin{aligned}
& m_p (\ddot{z}_n - 2\Omega_c \dot{\mathbf{h}}_n - \Omega_c^2 \mathbf{z}_n) - k_{sn} \mathbf{d}_{sn} \cos \mathbf{a} - k_{rn} \mathbf{d}_{rn} \cos \mathbf{a} - k_p \mathbf{d}_{nr} = 0 \\
\text{Planet n:} \quad & m_p (\ddot{\mathbf{h}}_n + 2\Omega_c \dot{\mathbf{z}}_n - \Omega_c^2 \mathbf{h}_n) - k_{sn} \mathbf{d}_{sn} \sin \mathbf{a} + k_{rn} \mathbf{d}_{rn} \sin \mathbf{a} - k_p \mathbf{d}_{nt} = 0 \\
& (I_p / r_p^2) \ddot{u}_n + k_{sn} \mathbf{d}_{sn} - k_{rn} \mathbf{d}_{rn} = 0
\end{aligned} \tag{5}$$

where T_r , T_c are the external torque's applied to the ring and carrier. The \mathbf{d} are compressions of the elastic elements and defined as:

$$\text{Sun-planet mesh:} \quad \mathbf{d}_{sn} = y_s \cos \mathbf{y}_{sn} - x_s \sin \mathbf{y}_{sn} - \mathbf{z}_n \sin \mathbf{a}_s - \mathbf{h}_n \cos \mathbf{a}_s + u_s + u_n + e_{sn} \tag{6}$$

$$\text{Ring-planet mesh:} \quad \mathbf{d}_{rn} = y_r \cos \mathbf{y}_{rn} - x_r \sin \mathbf{y}_{rn} - \mathbf{z}_n \sin \mathbf{a}_r + \mathbf{h}_n \cos \mathbf{a}_r + u_r - u_n + e_{rn} \tag{7}$$

$$\text{planet bearing radial:} \quad \mathbf{d}_{nr} = y_c \sin \mathbf{y}_n + x_c \cos \mathbf{y}_n - \mathbf{z}_n \tag{8}$$

$$\text{planet bearing tangent.} \quad \mathbf{d}_{nt} = y_c \cos \mathbf{y}_n - x_c \sin \mathbf{y}_n - \mathbf{h}_n + u_c \tag{9}$$

where $\mathbf{y}_m = \mathbf{y}_n + \mathbf{a}_r$ and \mathbf{a}_r is the pressure angle of the ring-planet mesh.

Equation (6) is derived from synthesis of the sun and planet deflections in the direction of the line of action for sun-planet meshes (Figure 3.a). Similarly, (7)-(9) are obtained by kinematics analyses of ring-planet meshes (Figure 3.b) and the planet bearing interfaces with the carrier (Figure 3.c)

Assembling the system equations in matrix form yields

$$\begin{aligned}
& M \ddot{\mathbf{q}} + \Omega_c G \dot{\mathbf{q}} + [K_b + K_m - \Omega_c^2 K_\Omega] \mathbf{q} = T(t) + F(t) \\
& \mathbf{q} = (x_c, y_c, u_c, x_r, y_r, u_r, x_s, y_s, u_s, \mathbf{z}_1, \mathbf{h}_1, u_1, \dots, \mathbf{z}_N, \mathbf{h}_N, u_N)
\end{aligned} \tag{10}$$

M is the inertia matrix and K_b is the bearing stiffness matrix. G and K_w result from high-speed carrier rotation and have not been included in published models. To model the time-varying stiffness associated with changing numbers of teeth in contact at each mesh, K_m can be decomposed into mean and time-varying components. Tooth separation nonlinearly is implicated included in $K_m(t)$. $t(t)$ are the applied external torque and $F(t)$ represents the static transmission error excitation.

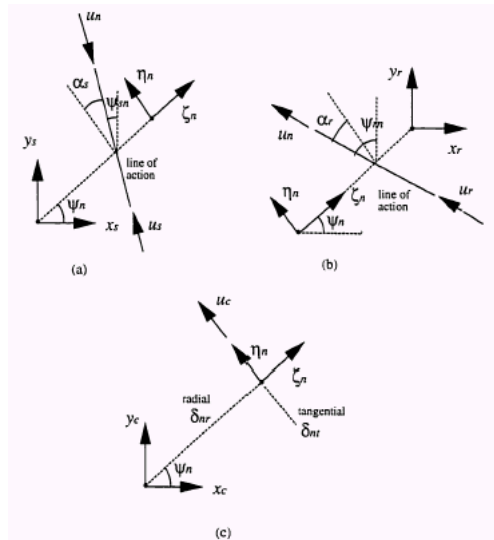


Figure 3. Kinematics sketches to derive relative component deflections

As an example the planetary gear in this paper is the system with four planets and 18 degrees of freedom. Model parameters of the planetary gear are given in Table 1.

Table 1. Model parameters of the planetary gear

	Sun	Ring	Carrier	Planet
Mass (kg)	0.4	2.35	5.43	0.66
I/r^2 (kg)	0.39	3.00	6.29	0.61
Base diameter(mm)	77.42	275.03	177.8	100.35
Teeth number	27	99		35
Mesh stiffness (N/m)		$k_{sp}=k_{rp}=k_m=$	5×10^8	
Bearing stiffness (N/m)		$k_p=k_s=k_r=k_c=$	10^8	
Torsion stiffness (N/m)		$k_{ru}=10^9$	$K_{su}=k_{cu}=0$	
Pressure angle ($^\circ$)		$\alpha_s=\alpha_r=\alpha=$	24.6	

The free vibration analysis calculates critical parameters such as natural frequencies and vibration modes that are essential for almost all-dynamic investigations. All the vibration modes are classified into rotational, translational and planet modes with distinctive properties. These well-defined properties are not valid when planets are arbitrarily spaced, but still apply to practically important case of diametrically opposed planets. The free vibration properties are very useful for future analyses of planetary gear dynamics, including eigensensitivity to design parameters, natural frequency veering, planet mesh phasing and parametric instabilities from mesh stiffness variations.

The natural frequency (example of four planet) for model parameter given in Table 1 is:

Table 2. Natural frequency for four planets

	Translation	Rotation	Planet	Translation	Rotation	Planet
Natural frequency (Hz)	769	1156	1609	1710	1781	2175

Figure 4 shows the spectrum of the steady state planet radial deflection for range of operating speeds. At all speeds, the response has frequency content only at mesh frequency and harmonics, although this is not imposed in the Finite element model. The sun rotational response has no spectral content in the odd harmonics of mesh frequency, and translational mode resonance's are absent in the remaining even harmonics.

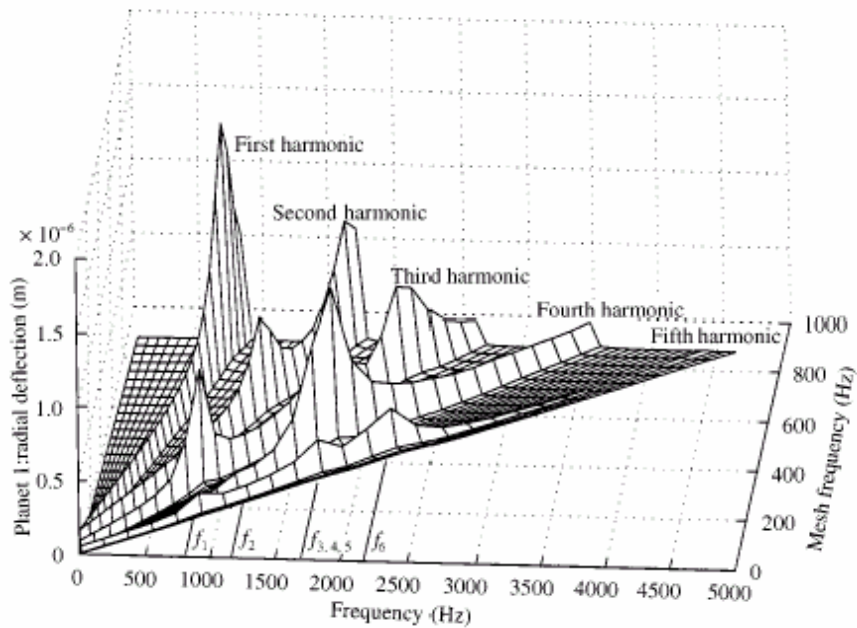


Figure 4. Easy state planet radial displacement spectrum for a range of operating speeds

The solutions are obtained from Numerical integration using mesh stiffness in rectangular waveforms as shown in Figure 5. The resonance excited by the primary instability $2\omega_5$ is extremely large because tooth separation (that is, vanishing mesh stiffness) is not considered; the mesh stiffness are pre-specified functions of time (Fig.5). In practice, tooth separation (clearance nonlinearly) occurs for large dynamic responses and its effects are dramatic. Sun-planet tooth separation $k_{sp}=0$ is apparent in Figure 6. For mesh frequency in the primary instability region of $2\omega_5$.

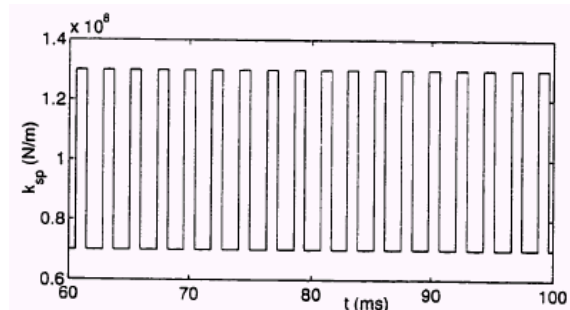


Figure 5. The sun-planet mesh stiffness is pre-specified

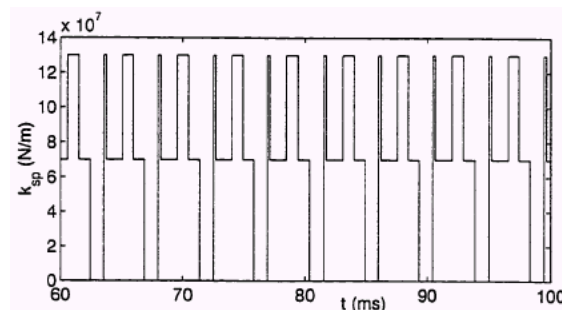


Figure 6. Sun-planet tooth separation ($k_{sp}=0$) occurs for $W=4.5 \text{ kHz}=2\omega_5$

Figure 7 shows a time signal of acceleration between sun and planet of planetary gear. Those results were simulated with MatLab ver 6 and theoretically expected.

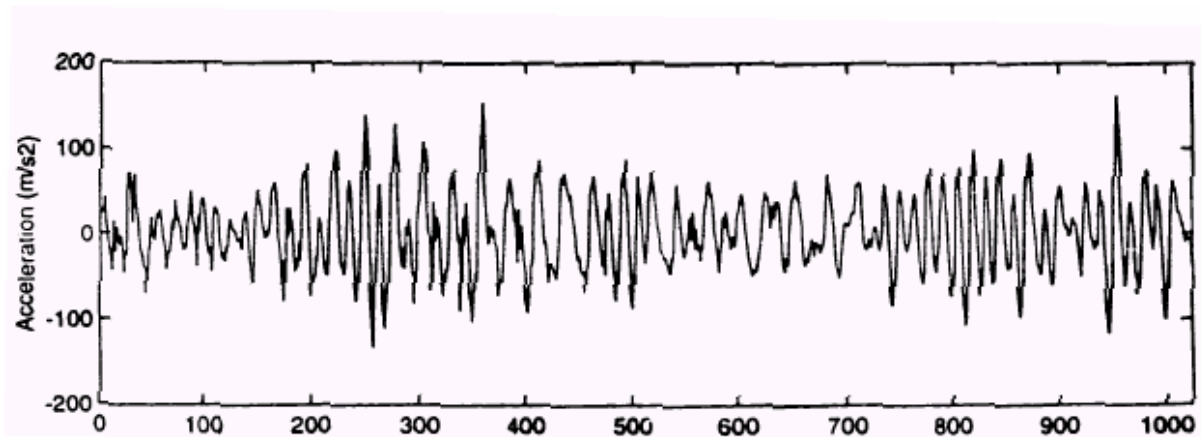


Figure 7. Sun-planet time signal of acceleration for N=1000 sample (125ms).

3. Conclusion

The scope of this study is to advance the modelling and understanding of planetary gear dynamics and analytically examine certain critical factors affecting planetary gear noise and vibration. This research focuses on the following specific task.

- Derive a lumped-parameter model for spur planetary gears, including different planet phasing, gyroscopic effects; mesh stiffness variation and transmission error excitation.
- Investigate the parametric instabilities caused by multiple time-varying mesh stiffness. Two-stage gear systems are examined first to clarify previous conflicts and derive simple expressions of instability boundaries. The well-defined modal properties are used to identify the effects of contact ratios and mesh phasing on planetary gear parametric instability.

References

Kahraman.A, Singh.R, "Nonlinear dynamics of a spur gear pair" , *Journal of sound and vibration*, 142(1),1990,pp.49-75.

Geramitcioski T.,Trajceviski Lj., "Dynamic model of a spur gear system",*International Symposium RIM-Revitalization and Modernization of Production*, 27-29,09.2001 Bihac, BiH

Lin J., " Analytical Investigation of Planetary Gear Dynamic" doctor dissertation presented in the Ohio State University in November 2000

Prof. dr. Tale Geramitcioski
 Faculty of Tehnical Sciences, Bitola
 Ivo Lola Ribar bb, Bitola,R.Macedonia
 Tel.:++389 47 31355
 Fax:++389 47 48320
 Email: tale.geramitcioski@uklo.edu.mk